sustainability

MDPI

Article

Evaluation of the Aging Properties of Terminal Blend Hybrid Asphalt Based on Chemical and Rheological Methods

Sheng Wang [1,2,*], Weidong Huang [1], Xueyan Liu [2] and Peng Lin [2]

[1] Key Laboratory of Road and Traffic Engineering of Ministry of Education, Tongji University, Tongda Building, 4800 Cao'an Road, Shanghai 201804, China; hwd@tongji.edu.cn

[2] Section of Pavement Engineering, Department of Engineering Structures, Faculty of Civil Engineering and Geosciences, Delft University of Technology, Stevinweg 1, 2628 CN Delft, The Netherlands; x.liu@tudelft.nl (X.L.); p.lin-2@tudelft.nl (P.L.)

* Correspondence: s.wang-13@tudelft.nl

Abstract: The chemical and rheological properties of terminal blend hybrid asphalt (TBHA) contributing to the consumption of waste tires before and after aging were studied. Styrene-butadiene-styrene (SBS) polymer, sulphur, crumb rubber (CR), and neat asphalt were chosen to prepare the TBHA. The short-term aging (STA) and long-term aging (LTA) of TBHA were simulated using a rolling thin film oven test (RTFOT) and pressure aging vessel (PAV), separately. The chemical and rheological properties of the TBHA were tested. The results show that the G* and G*/sin δ of TBHA ares generally lower than SBS-modified asphalt (SBSMA) at 76 °C, and the δ, $J_{nr}0.1$, and $J_{nr}3.2$ of TBHA are generally higher than SBSMA at 76 °C. Additionally, with the decrease of CR, the G* and G*/sin δ of TBHA decreased more obviously, and the G* and G*/sin δ of 5T_3S_0.2Sul (5 wt% CR, 3 wt% SBS, and 0.2 wt% sulphur) were the smallest. Moreover, during the STA, the SBS modifier in the TBHA degraded and made the bitumen predominantly soft; however, during the LTA, the hardening of the bitumen played a dominant role and increased its elasticity. The superior anti-aging properties of TBHA (both STA and LTA) are further demonstrated.

Keywords: terminal blend hybrid asphalt; rheological properties; short-term aging; long-term aging

check for updates

Citation: Wang, S.; Huang, W.; Liu, X.; Lin, P. Evaluation of the Aging Properties of Terminal Blend Hybrid Asphalt Based on Chemical and Rheological Methods. *Sustainability* **2022**, *14*, 7865. https://doi.org/10.3390/su14137865

Academic Editors: Edoardo Bocci and Rui Micaelo

Received: 2 May 2022
Accepted: 24 June 2022
Published: 28 June 2022

Publisher's Note: MDPI stays neutral with regard to jurisdictional claims in published maps and institutional affiliations.

Copyright: © 2022 by the authors. Licensee MDPI, Basel, Switzerland. This article is an open access article distributed under the terms and conditions of the Creative Commons Attribution (CC BY) license (https://creativecommons.org/licenses/by/4.0/).

1. Introduction

With the rapid development of the automotive industry, the amount of crumb rubber (CR) obtained from the treatment of waste tires is increasing. The use of CR in asphalt modification to enhance the road performance of asphalt is an effective resource utilization [1,2]. Crumb-rubber-modified asphalt (CRMA) not only makes use of a large number of waste tires and reduces pollution, but also has excellent high- and low-temperature properties, which can effectively extend the service life of pavements and reduce the occurrence of pavement distress [3–6]. The traditional CRMA preparation process is simple and fast, but at the same time, there are some drawbacks [7,8]. Firstly, as CR and asphalt are thermodynamically incompatible systems, in the CRMA preparation process, in order for the modified asphalt to achieve a certain performance, the amount of CR needs to be higher than 15%, resulting in the fact that the CR dispersed in the asphalt is difficult to form into a plastic mesh structure. The asphalt is quick to produce a segregation phenomenon, which is not conducive to long-term storage and transportation. Secondly, in the process of CR development and swelling, CR will absorb the light components in the asphalt, increasing the viscosity of CRMA, which requires a high temperature in order to facilitate the mixing of asphalt and minerals [9].

To solve the cost and difficulty of the construction of CR asphalt pavements, researchers have begun to investigate styrene-butadiene-styrene (SBS)/CR modified asphalt [10–12]. SBS modified asphalt (SBSMA) is a polymer-modified asphalt, and the storage stability of SBSMA has been improved through extensive research [13,14]. However, SBS is expensive

and the SBSMA produced by modifying the bitumen with SBS alone suffers from inadequate aging resistance. By combining CR and SBS, the aging resistance of the bitumen can be improved, and the amount of CR can be reduced, thus reducing the viscosity of the bitumen [10]. In addition, from a practical point of view, the SBS/CR-composite-modified asphalt pavement has a great advantage over SBSMA pavement in terms of reducing traffic noise and can make it possible to save part of the cost of sound insulation facilities in the construction of highways [15,16].

The terminal blend (TB) process provides a new technical approach to the production of CRMA from the perspective of high temperature degradation technology and improves the storage stability of CRMA [17]. This process allows CR and asphalt to be sheared at high temperatures for long periods at high speeds to produce modified bitumen, allowing a high degree of desulphurization and cracking of the CR [18], which can be stored uniformly and stably in the asphalt [19–22], effectively avoiding the storage stability problems associated with inadequate desulphurization of CR caused by insufficient degradation [23]. The CR-composite SBS-modified bitumen prepared under the TB process is called terminal blend hybrid asphalt (TBHA).

Thermal oxygen aging is one of the aging phenomena of asphalt produced by an oxidation reaction under high temperature conditions, and is divided into short-term aging (STA) (in the process of storage, transportation, and mixing) and long-term aging (LTA) (after the completion of asphalt paving) [24], which has a certain impact on the pavement performance and its life. In the actual use state of asphalt pavement, the asphalt will also be affected by ultraviolet rays from solar radiation, resulting in an aging reaction, leading to changes in its physical and chemical properties, which affect the service life of the pavement. Most of the research on TBHA has focused on the performance comparison of pre-aging asphalt [25], and the application of TBHA aging performance is still in the exploration stage [22,26]. The research on the aging performance of modified bitumen is mainly through the testing of penetration, ductility, and softening points to reflect the performance of modified bitumen after aging, but there is no in-depth research on the changes in TBHA chemical composition and rheological index during thermal oxygen aging. Therefore, in this study, the effect of aging on the chemical and rheological properties of TBHA was investigated. The changes before and after STA and LTA in the chemical composition of the TBHA were analyzed using the attenuated total reflection-Fourier transform infrared spectroscopy (ATR-FTIR) test. The rheological indexes of the TBHA binders were also evaluated. In addition, correlations between TBHA's chemical performance indexes and rheological performance indexes were studied.

2. Materials and Methods

2.1. Materials

In this paper, linear SBS polymer, sulphur, CR, and neat asphalt (PG 64-16) were selected to prepare the five kinds of TBHA. The details of the TBHA composition are present in Table 1. The softening point, ductility (10 °C), and penetration (25 °C) of neat asphalt are 52 °C, 25 cm, and 70d mm respectively. The choice of sulphur in this paper helps to ensure the homogeneity of the TBHA network structure. The linear SBS polymer has an average molecular weight of 120,000 g/mol. The −30 mesh CR, containing 54% natural rubber and synthetic rubber, was produced in Jiangyin, China. Sulphur was employed as a cross-linking agent to meet the storage stability requirements of TBHA. Figure 1 provides an illustration of the detailed preparation of TBHA.

Table 1. Description of Asphalt Studied.

Binder Type	Modification Plan		
	Linear SBS Polymer, %	Sulphur, %	CR, %
0T_3S_0.1Sul	3	0.1	0
5T_3S_0.2Sul	3	0.2	5
10T_3S_0.2Sul	3	0.2	10
15T_3S_0.2Sul	3	0.2	15
20T_3S_0.2Sul	3	0.2	20

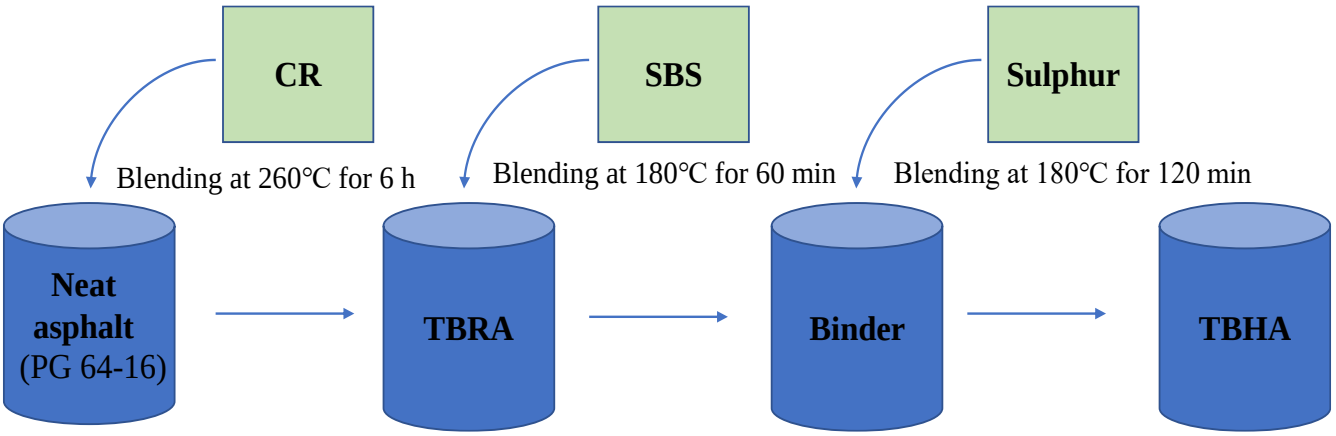


Figure 1. Schematic of the preparation of TBHA.

2.2. Aging Procedures

In the study, based on AASHTO T240 and AASHTO R28 [27,28], the binders were conditioned using the rolling thin-film oven (RTFO) test at 163 °C for 85 min to simulate the STA, and the obtained RTFO-aged binders were subsequently moved to the LTA process by pressure aging vessel (PAV) at 100 °C for 20 h.

2.3. ATR-FTIR Test

The chemical characteristics of TBHA before and after STA and LTA were measured using the ATR-FTIR test. The TBHA was subjected to 32 scans and the test range was 4000–600 cm^{-1}. Three replicates were used for each test, and the final data are the average value of every experiment.

The carbonyl and sulfoxide groups are two oxidation functional groups, but during aging, the sulfoxide group of the TBHA is less stable. Therefore, carbonyl groups were chosen to assess the oxidation degree of TBHA in this study. Higher I_{CA} values indicate greater oxidation of TBHA. The I_{CA} was calculated as shown in Table 2.

Table 2. Calculation Methods of I_{CA}.

Index	Calculation Method
I_{CA}	$CI= A_{1700cm^{-1}}/A_{2700\sim3000cm^{-1}}$

A (XX) cm^{-1} represents the area of (XX) cm^{-1} peak.

2.4. Temperature Sweep (TS) Test

The TS test was carried out on the TBHA with a 25 mm parallel plate and a 1 mm gap. The frequency (ω) was set at 10 rad/s. The sweeping temperature range was set at 76 °C. Complex modulus (G*), phase angle (δ), G*/sin δ, storage modulus (G′), loss modulus (G″), η″ values (η″ = G′/ω), and η′ values (η′ = G″/ω) were utilized to analyze the rheological performances of TBHA.

2.5. Multiple Stress Creep and Recovery (MSCR) Test

The MSCR test was performed according to AASHTO M332-14 in the dynamic shear rheometer (DSR) machine at 76 °C to get values of $J_{nr}0.1$, $J_{nr}3.2$, $J_{nr\text{-}diff}$, R0.1, R3.2, and R_{diff} [29]. $J_{nr}3.2$ and $J_{nr}0.1$ are used to indicate the amount of the non-recoverable creep compliance (J_{nr}) at 3.2 kPa and 0.1 kPa stress to reflect the elasticity of the binder. R3.2 and R0.1 are expressed in this article as the percent recovery (R) of TBHA under 3.2 kPa and 0.1 kPa, respectively.

3. Results and Discussion

3.1. ATR-FTIR Analysis

ΔI_{CA} is the difference in the change value of I_{CA} after STA and LTA, which is used to quantitatively evaluate the aging extent of TBHA. TBHA binders before and after STA and LTA were examined via ATR-FTIR, and the homologous I_{CA} and ΔI_{CA} are shown in Figure 2. As shown in Figure 2, from STA to LTA, the I_{CA} value continuously increases for the same binder, and the ΔI_{CA} of the TBHA binder is less than that of the 0T_3S_0.1Sul after the STA and LTA. The ΔI_{CA} ranking after STA is 5T_3S_0.2Sul < 20T_3S_0.2Sul < 15T_3S_0.2Sul < 10T_3S_0.2Sul < 0T_3S_0.1Sul. The ΔI_{CA} of 5T_3S_0.2Sul is the lowest. In addition, the ranking of ΔI_{CA} after LTA is 20T_3S_0.2Sul < 15T_3S_0.2Sul < 5T_3S_0.2Sul < 10T_3S_0.2Sul < 0T_3S_0.1Sul, indicating CR can delay the effect of STA and LTA compared with 0T_3S_0.1Sul, and the superior anti-aging properties of TBHA (both STA and LTA) are further demonstrated. The reason for this is that nano-silica in the CR of TBHA enters the asphalt after desulfurization and degradation and acts as an oxygen barrier and insulator, which improves the aging resistance of the asphalt [30–33]. Thus, the nano-silica in the TBRA binder makes its resistance of STA and LTA better than that of 0T_3S_0.1Sul.

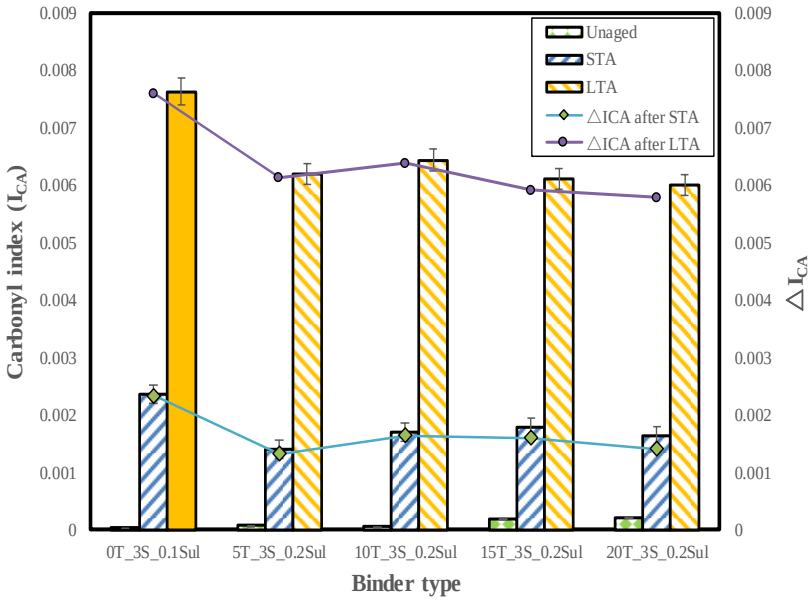


Figure 2. I_{CA} and ΔI_{CA} of TBHA at unaged and aged conditions.

*3.2. Evaluation of G**

Figure 3 shows the G* of TBHA at 76 °C. As shown in Figure 3, the G* of 0T_3S_0.1Sul, 5T_3S_0.2Sul, 10T_3S_0.2Sul, 15T_3S_0.2Sul, and 20T_3S_0.2Sul in virgin condition are 1375, 1115, 1240, 1233, and 1302 Pa respectively. In other words, the G* value ranking of binders in unaged condition is 0T_3S_0.1Sul > 20T_3S_0.2Sul > 10T_3S_0.2Sul > 15T_3S_0.2Sul > 5T_3S_0.2Sul. The above results show that the G* of TBHA is generally lower than 0T_3S_0.1Sul at 76 °C. With the decrease of CR, the G* of TBHA decreases more obviously, and the G* of 5T_3S_0.2Sul is the smallest. This is due to the high temperature desulphurization degradation of CR, which greatly reduces the effect of CR on the mechanical

properties of TBHA, leading to a reduction in G*, and a smaller G* value for TBHA with a smaller CR doping. However, the addition of SBS followed by the sulphur cross-linking agent to the desulphurized and degraded TBHA system results in a cross-linking reaction, leading to an increase in G* as the CR dosing increases [15].

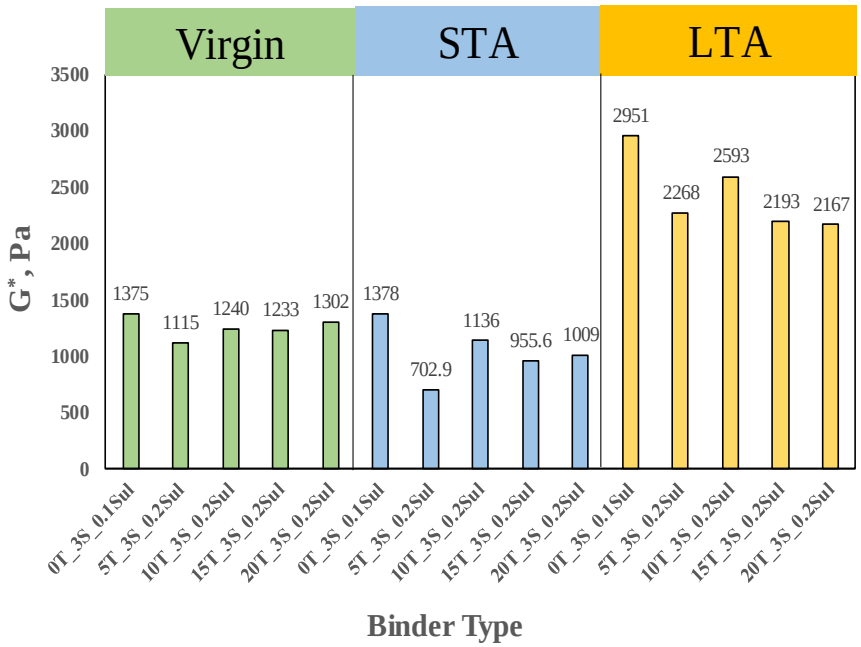


Figure 3. G* of TBHA binders before and after aging.

The G* of 0T_3S_0.1Sul, 5T_3S_0.2Sul, 10T_3S_0.2Sul, 15T_3S_0.2Sul, and 20T_3S_0.2Sul in STA are 1378, 702.9, 1136, 955.6, and 1009 Pa respectively. Moreover, the G* of 0T_3S_0.1Sul, 5T_3S_0.2Sul, 10T_3S_0.2Sul, 15T_3S_0.2Sul, and 20T_3S_0.2Sul in LTA is 2951, 2268, 2593, 2193, and 2167 Pa respectively. The G* ranking of binders is 0T_3S_0.1Sul > 10T_3S_0.2Sul > 20T_3S_0.2Sul > 15T_3S_0.2Sul > 5T_3S_0.2Sul in STA condition, and the G* ranking values of binders is 0T_3S_0.1Sul > 10T_3S_0.2Sul > 5T_3S_0.2Sul > 15T_3S_0.2Sul > 20T_3S_0.2Sul in LTA condition. Compared to other TBHA binders, G* of 0T_3S_0.1Sul is the largest after experiencing both STA and LTA. The above results show that the G* of TBHA decreases after STA but becomes larger after LTA. The reason for this is that aging causes degradation of the SBS modifier in the TBHA, which softens the bitumen and weakens the age-hardening effect of the TBHA after STA [34–36], leading to a reduction in the G* growth rate. Additionally, different CR doping provides TBHA with different mechanical strength, resulting in different TBHA's G* at STA and LTA conditions. However, during the LTA aging phase, the age-hardening effect of TBHA plays a dominant role, increasing elasticity and G*.

3.3. Evaluation of δ

The δ values for TBHA are shown in Figure 4. As shown in Figure 4, the δ of 0T_3S_0.1Sul, 5T_3S_0.2Sul, 10T_3S_0.2Sul, 15T_3S_0.2Sul, and 20T_3S_0.2Sul in virgin condition are 67.95, 70.14, 69.24, 67.9, and 66.09°, respectively. The above results show that the δ of TBHA is generally higher than 0T_3S_0.1Sul at 76 °C, except 20T_3S_0.2Sul and 15T_3S_0.2Sul. The δ of 0T_3S_0.1Sul, 5T_3S_0.2Sul, 10T_3S_0.2Sul, 15T_3S_0.2Sul, and 20T_3S_0.2Sul in STA are 75.79, 84.97, 76.87, 79.11, and 75.35°, respectively. Moreover, the δ of 0T_3S_0.1Sul, 5T_3S_0.2Sul, 10T_3S_0.2Sul, 15T_3S_0.2Sul, and 20T_3S_0.2Sul in LTA is 78.89, 76.84, 75.52, 77.83, and 75.36°, respectively. The δ ranking of binders is 5T_3S_0.2Sul > 15T_3S_0.2Sul > 10T_3S_0.2Sul > 0T_3S_0.1Sul > 20T_3S_0.2Sul in STA condition, and the ranking of δ values of TBHA is 0T_3S_0.1Sul > 15T_3S_0.2Sul > 5T_3S_0.2Sul > 10T_3S_0.2Sul > 20T_3S_0.2Sul in LTA condition. The results show that δ increases after

STA for TBHA and becomes smaller after LTA, which is the opposite of the rule after G* aging, indicating that TBHA softens and then hardens from STA to LTA.

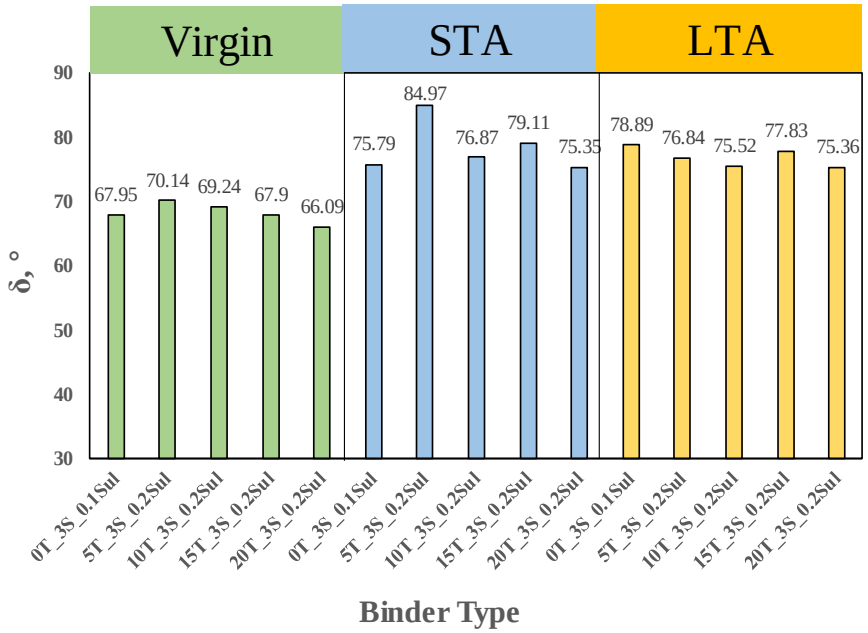


Figure 4. δ of TBHA binders before and after aging.

3.4. Evaluation of G/sin δ*

The G*/sin δ of TBHA is summarized in Figure 5. The G*/sin δ of 0T_3S_0.1Sul, 5T_3S_0.2Sul, 10T_3S_0.2Sul, 15T_3S_0.2Sul, and 20T_3S_0.2Sul in virgin condition are 1484, 1186, 1326, 1331, and 1424 Pa, respectively. The above results show that the G*/sin δ of TBHA has decreased compared to 0T_3S_0.1Sul. The G*/sin δ sequence of TBHA after aging is the same as that of G*. The G*/sin δ of TBHA decreases after STA and becomes larger after LTA.

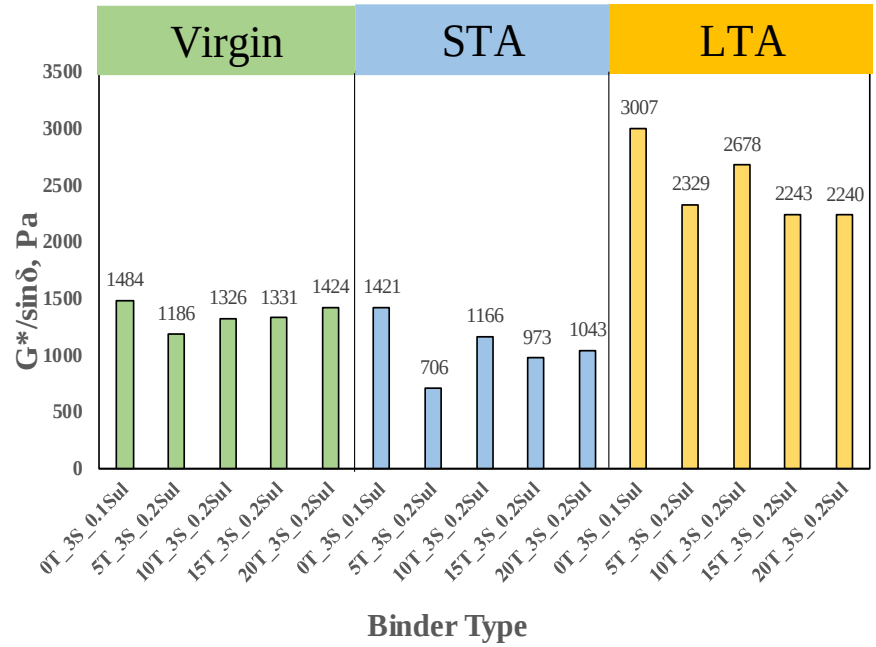


Figure 5. G*/sin δ of TBHA binders before and after aging.

3.5. Evaluation of G′, G″, η′, and η″

G′ represents the energy stored and releasable by the material under alternating stress, reflecting the elastic component of the bitumen. The G″ reflects the energy dissipated in the form of heat due to internal friction during deformation, reflecting the viscous component of the bitumen. Considering the modified bitumen as a linear viscoelastic body, the complex viscosity (η) obtained under stress can be broken down into two parts: one part is the imaginary part η′ of the complex viscosity, which represents the contribution of the purely elastic part of the modified bitumen. The other part is the real part η″ of the complex viscosity, representing the contribution of the pure viscous part of the modified bitumen. The G′ and G″ of binders before and after STA and LTA are presented in Table 3, and η′ and η″ of binders before and after STA and LTA are shown in Table 4. In Table 3, the G* of 20T_3S_0.2Sul is higher than that of the other TBHA at virgin status. The ranking of binders' G′ at virgin status is 5T_3S_0.2Sul < 10T_3S_0.2Sul < 15T_3S_0.2Sul < 0T_3S_0.1Sul < 20T_3S_0.2Sul, and the ranking of binders' G″ at virgin status is 5T_3S_0.2Sul < 15T_3S_0.2Sul < 10T_3S_0.2Sul < 20T_3S_0.2Sul < 0T_3S_0.1Sul. The G′ and G″ of binders are in the same order at STA status, which is 5T_3S_0.2Sul < 15T_3S_0.2Sul < 20T_3S_0.2Sul < 10T_3S_0.2Sul < 0T_3S_0.1Sul, indicating that at STA status, the elastic component and the viscous component of the bitumen is less than that of 0T_3S_0.1Sul. As the aging level changes from STA to LTA, the G′ and G″ of the binders become larger, indicating the elastic component and the viscous component of the TBHA and 0T_3S_0.1Sul become larger from STA to LTA. In addition, the G′ and G″ of TBHA binders at STA status are also less than that of TBHA binders at virgin status. The η′ and η″ of TBHA before and after STA and LTA are presented in Table 4. For the same binder at virgin status, STA status, and LTA status, the rule of variation of G′ coincides with the rule of variation of its η″, and the rule of change in G″ is the same as that of η′. The above results show that from virgin status to LTA status, the elastic component and the viscous component of the TBHA and 0T_3S_0.1Sul decrease and then increase. This is due to the increased asphaltene in the TBHA and 0T_3S_0.1Sul after aging.

Table 3. G′ and G″ of Binders.

Binder Type	Virgin Status				STA Status				LTA Status			
	G′, Pa	Rank	G″, Pa	Rank	G′, Pa	Rank	G″, Pa	Rank	G′, Pa	Rank	G″, Pa	Rank
0T_3S_0.1Sul	516	2	1274	1	338	1	1336	1	569	2	2896	1
5T_3S_0.2Sul	379	5	1049	5	62	5	700	5	516	4	2208	3
10T_3S_0.2Sul	440	4	1159	3	258	2	1106	2	648	1	2511	2
15T_3S_0.2Sul	464	3	1142	4	181	4	938	4	462	5	2144	4
20T_3S_0.2Sul	528	1	1190	2	255	3	976	3	548	3	2097	5

Table 4. η′ and η″ of Binders.

Binder Type	Virgin Status				STA Status				LTA Status			
	η′, Pa·s	Rank	η″, Pa·s	Rank	η′, Pa·s	Rank	η″, Pa·s	Rank	η′, Pa·s	Rank	η″, Pa·s	Rank
0T_3S_0.1Sul	127.4	1	51.6	2	133.6	1	33.8	1	289.6	1	56.9	2
5T_3S_0.2Sul	104.9	5	37.9	5	70.0	5	6.2	5	220.8	3	51.6	4
10T_3S_0.2Sul	115.9	3	44.0	4	110.6	2	25.8	2	251.1	2	64.8	1
15T_3S_0.2Sul	114.2	4	46.4	3	93.8	4	18.1	4	214.4	4	46.2	5
20T_3S_0.2Sul	119.0	2	52.8	1	97.6	3	25.5	3	209.7	5	54.8	3

3.6. Evaluation of $J_{nr}0.1$ and $J_{nr}3.2$

The J_{nr} index correlates well with the high-temperature performance of asphalt mixes. lower J_{nr} values indicate better resistance to high temperature rutting [37]. J_{nr} at 0.1 and 3.2 kPa were recorded as $J_{nr}0.1$ and $J_{nr}3.2$. As shown in Figures 6 and 7, the sequence of $J_{nr}0.1$ and $J_{nr}3.2$ of TBHA before and after STA and LTA is the same as that of δ. The $J_{nr}0.1$ and $J_{nr}3.2$ of TBHA are generally higher than 0T_3S_0.1Sul at 76 °C, and the $J_{nr}0.1$ and $J_{nr}3.2$ of TBHA increase after STA and become smaller after LTA.

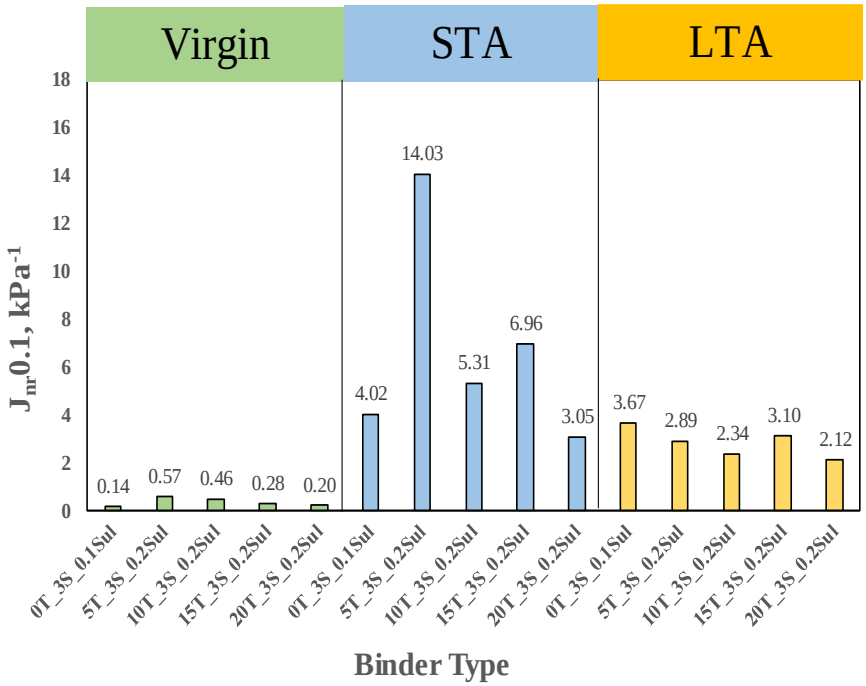


Figure 6. $J_{nr}0.1$ of TBHA binders before and after aging.

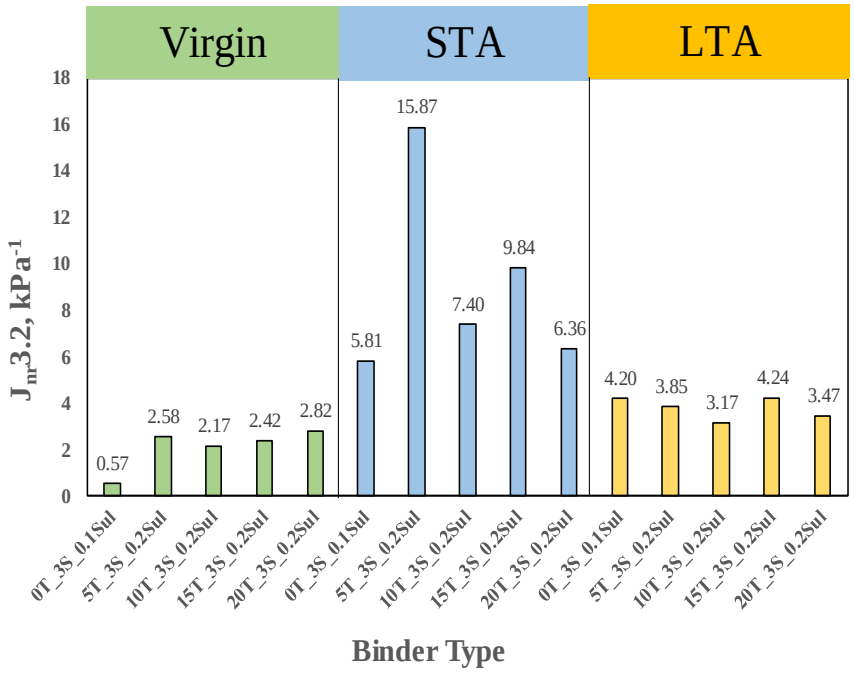


Figure 7. $J_{nr}3.2$ of TBHA binders before and after aging.

3.7. Evaluation of R0.1, R3.2, $J_{nr\text{-}diff}$, and R_{diff}

The higher the R value, the higher the elastic deformation capacity of the asphalt material. R0.1 and R3.2 of binders at virgin status, STA status, and LTA status are presented in Table 5, which shows that the R0.1 and R3.2 of the same binder decrease from virgin status to LTA status. The R0.1 and R3.2 of TBHA at virgin status are lower than that of 0T_3S_0.1Sul. In addition, the ranking of R0.1 and R3.2 at STA status both are 5T_3S_0.2Sul < 15T_3S_0.2Sul < 10T_3S_0.2Sul < 0T_3S_0.1Sul < 20T_3S_0.2Sul, and the ranking of R0.1 and R3.2 at LTA status both are 0T_3S_0.1Su l < 15T_3S_0.2Sul < 5T_3S_0.2Sul < 10T_3S_0.2Sul < 20T_3S_0.2Sul, which indicates that compared with 0T_3S_0.1Sul, aging has less impact on the percent recovery of TBHA. This is due to the fact that CR in TBHA can have an oxygen-barrier effect to improve its aging resistance.

Table 5. R0.1 and R3.2 of Binders.

Binder Type	Virgin Status				STA Status				LTA Status			
	R0.1, %	Rank	R3.2, %	Rank	R0.1, %	Rank	R3.2, %	Rank	R0.1, %	Rank	R3.2, %	Rank
0T_3S_0.1Sul	96.57	1	84.36	1	28.58	2	10.12	2	3.35	5	2.88	5
5T_3S_0.2Sul	89.17	5	51.75	2	0	5	0	5	18.78	3	5.39	3
10T_3S_0.2Sul	89.95	4	51.73	3	22.88	3	5.76	3	21.77	2	6.91	2
15T_3S_0.2Sul	93.50	3	45.92	4	20.47	4	2.54	4	18.63	4	4.23	4
20T_3S_0.2Sul	95.00	2	37.50	5	55.14	1	12.90	1	37.31	1	9.60	1

The stress sensitivity index ($J_{nr\text{-}diff}$, and R_{diff}) reflects the sensitivity of the mechanical response of the bituminous material to different stress levels, and the higher the stress sensitivity index, the more significant the non-linear characteristics of the material during the transition from low- to high-stress levels. $J_{nr\text{-}diff}$ and R_{diff} of binders at virgin status, STA status, and LTA status are shown in Table 6. As illustrated in Table 6, the $J_{nr\text{-}diff}$ values of all TBHA show a decreasing trend from virgin status to LTA status, indicating that aging reduces the stress sensitivity of TBHA to J_{nr}. In addition, R_{diff} values become bigger from virgin status to LTA status. This indicates that the stress sensitivity of the R of TBHA increases after LTA. This is because, after LTA, SBS undergoes degradation and CR acts as a skeleton in TBHA, resulting in an increased stress sensitivity of TBHA.

Table 6. $J_{nr\text{-}diff}$ and R_{diff} of Binders.

Binder Type	Virgin Status				STA Status				LTA Status			
	$J_{nr\text{-}diff}$, %	Rank	R_{diff}, %	Rank	$J_{nr\text{-}diff}$, %	Rank	R_{diff}, %	Rank	$J_{nr\text{-}diff}$, %	Rank	R_{diff}, %	Rank
0T_3S_0.1Sul	294.00	5	12.64	5	44.67	4	64.60	4	14.38	5	14.18	5
5T_3S_0.2Sul	349.18	4	41.97	4	13.08	5	0	5	33.19	4	71.31	3
10T_3S_0.2Sul	366.93	3	42.49	3	39.30	2	74.80	3	35.49	3	68.27	4
15T_3S_0.2Sul	752.97	2	50.89	2	41.27	2	87.62	1	36.66	2	77.30	1
20T_3S_0.2Sul	1280.95	1	60.52	1	108.60	1	76.61	2	63.85	1	74.26	2

3.8. Correlation Analysis

In order to further study the relationship between TBHA chemical and rheological indexes before and after STA and LTA, Pearson correlation analysis was carried out using SPSS software. The Pearson correlation of TBHA chemical and rheological indexes before and after STA and LTA are presented in Table 7. As shown in Table 7, there are good correlations between I_{CA}, G*, G″, and η′, and good correlations between G*, G*/sin δ, G″, and η′. However, the correlations between G*, $J_{nr}0.1$, $J_{nr}3.2$, $J_{nr\text{-}diff}$, R0.1, R3.2, and R_{diff} are not high, indicating that the rheological indexes of the DSR oscillation test and MSCR test index of TBHA binders before and after STA and LTA are not well correlated, and the rheological indexes of the DSR oscillation test and I_{CA} indexes of the ATR-FTIR test of TBHA before and after STA and LTA are better correlated.

Table 7. Pearson Correlation Analysis Results Index.

Index Type		I_{CA}	G*	δ	G*/sin δ	G′	G″	η′	η″	$J_{nr}0.1$	$J_{nr}3.2$	$J_{nr\text{-}diff}$	R0.1	R3.2	R_{diff}
I_{CA}	P	1	0.902	0.518	0.882	0.463	0.918	0.918	0.463	0.080	−0.050	−0.543	−0.709	−0.650	0.205
	N	15	15	15	15	15	15	15	15	15	15	15	15	15	15
G*	P	0.902	1	0.145	0.999	0.776	0.999	0.999	0.776	−0.276	−0.421	−0.277	−0.389	−0.307	0.068
	N	15	15	15	15	15	15	15	15	15	15	15	15	15	15
δ	P	0.518	0.145	1	0.099	−0.494	0.187	0.187	−0.494	0.865	0.799	−0.781	−0.945	−0.842	−0.002
	N	15	15	15	15	15	15	15	15	15	15	15	15	15	15
G*/sin δ	P	0.882	0.999	0.099	1	0.805	0.996	0.996	0.805	−0.314	−0.458	−0.238	−0.346	−0.267	0.062
	N	15	15	15	15	15	15	15	15	15	15	15	15	15	15
G′	P	0.463	0.776	−0.494	0.805	1	0.747	0.747	1.000	−0.752	−0.846	0.253	0.250	0.266	0.046
	N	15	15	15	15	15	15	15	15	15	15	15	15	15	15
G″	P	0.918	0.999	0.187	0.996	0.747	1	1.000	0.747	−0.240	−0.386	−0.313	−0.427	−0.343	0.073
	N	15	15	15	15	15	15	15	15	15	15	15	15	15	15
η′	P	0.918	0.999	0.187	0.996	0.747	1.000	1	0.747	−0.240	−0.386	−0.313	−0.427	−0.343	0.073
	N	15	15	15	15	15	15	15	15	15	15	15	15	15	15
η″	P	0.463	0.776	−0.494	0.805	1.000	0.747	0.747	1	−0.752	−0.846	0.253	0.250	0.266	0.046
	N	15	15	15	15	15	15	15	15	15	15	15	15	15	15
$J_{nr}0.1$	P	0.080	−0.276	0.865	−0.314	−0.752	−0.240	−0.240	−0.752	1	0.976	−0.495	−0.715	−0.620	−0.215
	N	15	15	15	15	15	15	15	15	15	15	15	15	15	15
$J_{nr}3.2$	P	−0.050	−0.421	0.799	−0.458	−0.846	−0.386	−0.386	−0.846	0.976	1	−0.395	−0.626	−0.607	−0.111
	N	15	15	15	15	15	15	15	15	15	15	15	15	15	15
$J_{nr\text{-}diff}$	P	−0.543	−0.277	−0.781	−0.238	0.253	−0.313	−0.313	0.253	−0.495	−0.395	1	0.759	0.558	−0.069
	N	15	15	15	15	15	15	15	15	15	15	15	15	15	15
R0.1	P	−0.709	−0.389	−0.945	−0.346	0.250	−0.427	−0.427	0.250	−0.715	−0.626	0.759	1	0.908	−0.124
	N	15	15	15	15	15	15	15	15	15	15	15	15	15	15
R3.2	P	−0.650	−0.307	−0.842	−0.267	0.266	−0.343	−0.343	0.266	−0.620	−0.607	0.558	0.908	1	−0.393
	N	15	15	15	15	15	15	15	15	15	15	15	15	15	15
R_{diff}	P	0.205	0.068	−0.002	0.062	0.046	0.073	0.073	0.046	−0.215	−0.111	−0.069	−0.124	−0.393	1
	N	15	15	15	15	15	15	15	15	15	15	15	15	15	15

4. Conclusions

The chemical and rheological properties of TBHA before and after STA and LTA were studied. The following conclusions were drawn:

- ATR-FTIR analysis shows the ΔI_{CA} of the TBHA binder is less than that of the 0T_3S_0.1Sul after the STA and LTA, and the superior anti-aging properties of TBHA (both STA and LTA) are further demonstrated.
- During the STA, the SBS modifier in the TBHA degrades and makes the bitumen predominantly soft, however, during the LTA, the hardening of the bitumen plays a dominant role and increases its elasticity.
- Before and after STA and LTA, the rheological indexes of the DSR oscillation test and the MSCR test indexes of the TBHA binder do not correlate well, but the rheological indexes of the DSR oscillation test and the I_{CA} indexes of the ATR-FTIR test of the TBHA binder correlate better.

Author Contributions: Conceptualization, S.W.; methodology, S.W.; validation, W.H.; investigation, X.L.; writing—original draft, S.W.; writing—review and editing, P.L.; visualization, P.L.; supervision, S.W. All authors have read and agreed to the published version of the manuscript.

Funding: This research was developed within the Projects of National Natural Science Foundation of China under grant number 51978518 and the China Scholarship Council (CSC No. 202106260114).

Institutional Review Board Statement: Not applicable.

Informed Consent Statement: Not applicable.

Data Availability Statement: The data presented in this study are available on request from the corresponding author.

Acknowledgments: The authors would like to express their appreciation for financial support from the National Natural Science Foundation of China under grant number 51978518. In addition, the first author acknowledges financial support from the China Scholarship Council (CSC No. 202106260114).

Conflicts of Interest: No potential conflict of interest was reported by the authors.

References

1. Lo Presti, D.; Izquierdo, M.A.; Jiménez del Barco Carrión, A. Towards storage-stable high-content recycled tyre rubber modified bitumen. *Constr. Build. Mater.* **2018**, *172*, 106–111. [CrossRef]
2. Sienkiewicz, M.; Borzędowska-Labuda, K.; Wojtkiewicz, A.; Janik, H. Development of methods improving storage stability of bitumen modified with ground tire rubber: A review. *Fuel Process. Technol.* **2017**, *159*, 272–279. [CrossRef]
3. Szerb, E.I.; Nicotera, I.; Teltayev, B.; Vaiana, R.; Rossi, C.O. Highly stable surfactant-crumb rubber-modified bitumen: NMR and rheological investigation. *Road Mater. Pavement Des.* **2018**, *19*, 1192–1202. [CrossRef]
4. Bressi, S.; Fiorentini, N.; Huang, J.; Losa, M. Crumb Rubber Modifier in Road Asphalt Pavements: State of the Art and Statistics. *Coatings* **2019**, *9*, 384. [CrossRef]
5. Hosseinnezhad, S.; Kabir, S.F.; Oldham, D.; Mousavi, M.; Fini, E.H. Surface functionalization of rubber particles to reduce phase separation in rubberized asphalt for sustainable construction. *J. Clean. Prod.* **2019**, *225*, 82–89. [CrossRef]
6. Tahami, S.A.; Mirhosseini, A.F.; Dessouky, S.; Mork, H.; Kavussi, A. The use of high content of fine crumb rubber in asphalt mixes using dry process. *Constr. Build. Mater.* **2019**, *222*, 643–653. [CrossRef]
7. Hemida, A.; Abdelrahman, M. Component analysis of bio-asphalt binder using crumb rubber modifier and guayule resin as an innovative asphalt replacer. *Resour. Conserv. Recycl.* **2021**, *169*, 105486. [CrossRef]
8. Kabir, S.F.; Zheng, R.; Delgado, A.G.; Fini, E.H. Use of microbially desulfurized rubber to produce sustainable rubberized bitumen. *Resour. Conserv. Recycl.* **2021**, *164*, 105144. [CrossRef]
9. Picado-Santos, L.G.; Capitão, S.D.; Neves, J.M.C. Crumb rubber asphalt mixtures: A literature review. *Constr. Build. Mater.* **2020**, *247*, 118577. [CrossRef]
10. Xiang, L.; Cheng, J.; Kang, S. Thermal oxidative aging mechanism of crumb rubber/SBS composite modified asphalt. *Constr. Build. Mater.* **2015**, *75*, 169–175. [CrossRef]
11. Dong, F.; Yu, X.; Liu, S.; Wei, J. Rheological behaviors and microstructure of SBS/CR composite modified hard asphalt. *Constr. Build. Mater.* **2016**, *115*, 285–293. [CrossRef]
12. Jiang, Z.; Easa, S.M.; Hu, C.; Zheng, X. Understanding damping performance and mechanism of crumb rubber and styrene-butadiene-styrene compound modified asphalts. *Constr. Build. Mater.* **2019**, *206*, 151–159. [CrossRef]
13. Tur Rasool, R.; Hongru, Y.; Hassan, A.; Wang, S.; Zhang, H. In-field aging process of high content SBS modified asphalt in porous pavement. *Polym. Degrad. Stab.* **2018**, *155*, 220–229. [CrossRef]
14. Shirini, B.; Imaninasab, R. Performance evaluation of rubberized and SBS modified porous asphalt mixtures. *Constr. Build. Mater.* **2016**, *107*, 165–171. [CrossRef]
15. Lin, P.; Huang, W.; Tang, N.; Xiao, F. Performance characteristics of Terminal Blend rubberized asphalt with SBS and polyphosphoric acid. *Constr. Build. Mater.* **2017**, *141*, 171–182. [CrossRef]
16. Li, B.; Huang, W.; Tang, N.; Hu, J.; Lin, P.; Guan, W.; Xiao, F.; Shan, Z. Evolution of components distribution and its effect on low temperature properties of terminal blend rubberized asphalt binder. *Constr. Build. Mater.* **2017**, *136*, 598–608. [CrossRef]
17. Han, L.; Zheng, M.; Wang, C. Current status and development of terminal blend tyre rubber modified asphalt. *Constr. Build. Mater.* **2016**, *128*, 399–409. [CrossRef]
18. Zeinali, A.; Blankenship, P.B.; Mahboub, K.C. Comparison of Performance Properties of Terminal Blend Tire Rubber and Polymer Modified Asphalt Mixtures. In Proceedings of the Second Transportation & Development Congress 2014, Orlando, FL, USA, 8–11 June 2014; American Society of Civil Engineers: Reston, VA, USA, 2014; pp. 239–248.
19. Jones, D.; Harvey, J.T.; Monismith, C.L. Reflective cracking study: Summary report. *Inst. Transp. Stud. Work. Pap. Ser.* 2008. Available online: https://escholarship.org/uc/item/357679nm (accessed on 1 May 2022).
20. Santucci, L. Rubber roads: Waste tires find a home. *Pavement Technol. Updat.* **2009**, *1*, 12.
21. Qi, X.; Shenoy, A.; Al-Khateeb, G.; Arnold, T.; Gibson, N.; Youtcheff, J.; Harman, T. Laboratory characterization and full-scale accelerated performance testing of crumb rubber asphalts and other modified asphalt systems. In Proceedings of the Asphalt Rubber 2006 Conference, Palm Springs, CA, USA, 25–27 October 2006; pp. 39–65.
22. Chipps, J.F.; Davison, R.R.; Glover, C.J. A model for oxidative aging of rubber-modified asphalts and implications to performance analysis. *Energy Fuels* **2001**, *15*, 637–647. [CrossRef]
23. Attia, M.; Abdelrahman, M. Enhancing the performance of crumb rubber-modified binders through varying the interaction conditions. *Int. J. Pavement Eng.* **2009**, *10*, 423–434. [CrossRef]

24. Crucho, J.; Picado-Santos, L.; Neves, J.; Capitão, S.; Al-Qadi, I.L. Tecnico accelerated ageing (TEAGE)–a new laboratory approach for bituminous mixture ageing simulation. *Int. J. Pavement Eng.* **2020**, *21*, 753–765. [CrossRef]
25. Ruan, Y.; Davison, R.R.; Glover, C.J. Oxidation and viscosity hardening of polymer-modified asphalts. *Energy Fuels* **2003**, *17*, 991–998. [CrossRef]
26. Airey, G.D. State of the Art Report on Ageing Test Methods for Bituminous Pavement Materials. *Int. J. Pavement Eng.* **2003**, *4*, 165–176. [CrossRef]
27. *AASHTO T240*; Standard Method of Test for Effect of Heat and Air on a Moving Film of Asphalt Binder (Rolling Thin-Film Oven Test). American Association of State Highway and Transportation Official: Washington, DC, USA, 2013.
28. *AASHTO R28*; Standard Practice for Accelerated Aging of Asphalt Binder Using a Pressurized Aging Vessel (PAV). American Association of State Highway and Transportation Official: Washington, DC, USA, 2012.
29. *AASHTO M 332-14*; Standard Specification for Performance-Graded Asphalt Binder using Multiple Stress Creep Recovery (MSCR) Test. American Association of State Highway and Transportation Official: Washington, DC, USA, 2014.
30. Hajj, E.Y.; Sebaaly, P.E.; Hitti, E.; Borroel, C. Performance Evaluation of Terminal Blend Tire Rubber HMA and WMA Mixtures-Case Studies. *J. Assoc. Asph. Paving Technol.* **2011**, *80*, 665–696.
31. Liu, L.; Li, M.; Lu, Q. Two-Step Mixing Process Elaboration of the Hot-Mix Asphalt Mixture Based on Surface Energy Theory. *J. Mater. Civ. Eng.* **2020**, *32*, 04020301. [CrossRef]
32. Wang, S.; Huang, W. Investigation of aging behavior of terminal blend rubberized asphalt with SBS polymer. *Constr. Build. Mater.* **2021**, *267*, 120870. [CrossRef]
33. Li, M.; Liu, L.; Xing, C.; Liu, L.; Wang, H. Influence of rejuvenator preheating temperature and recycled mixture's curing time on performance of hot recycled mixtures. *Constr. Build. Mater.* **2021**, *295*, 123616. [CrossRef]
34. Li, M.; Xing, C.; Liu, L.; Huang, W.; Meng, Y. Gel permeation chromatography-based method for assessing the properties of binders in reclaimed asphalt pavement mixtures. *Constr. Build. Mater.* **2022**, *316*, 126005. [CrossRef]
35. Zhang, H.; Cao, J.; Duan, H.; Luo, H.; Liu, X. Molecular dynamics insight into the adsorption and distribution of bitumen subfractions on Na-montmorillonite surface. *Fuel* **2022**, *310*, 122380. [CrossRef]
36. Yang, X.; Zhang, H.; Zheng, W.; Chen, Z.; Shi, C. A Novel Rejuvenating Method for Structural and Performance Recovery of Aged SBS-Modified Bitumen. *ACS Sustain. Chem. Eng.* **2022**, *10*, 1565–1577. [CrossRef]
37. D'Angelo, J.A. The Relationship of the MSCR Test to Rutting. *Road Mater. Pavement Des.* **2009**, *10*, 61–80. [CrossRef]